

## **Simultaneous and precise measurements of thermal, electrical and acoustic properties—new feature of the 403K phase transition in BaTiO<sub>3</sub>**

Akira Kojima<sup>1</sup>, Hiroshi Sasou<sup>1</sup>, Ken-ichi Tozaki<sup>2</sup>, Takuya Okazaki<sup>2</sup>, Yukio Yoshimura<sup>3</sup>, Naotoshi Tokunaga<sup>3</sup>, and Hiroshi Iwasaki<sup>3</sup>

- 1) Department of Materials Science, The University of Shiga Prefecture, Hikone, Shiga 522-8533, Japan
- 2) Department of Physics, Faculty of Education, Chiba University, Inage, Chiba 263-8522, Japan
- 3) Faculty of Science and Engineering, Ritsumeikan University, Kusatsu, Shiga 525-8577, Japan

In order to research phase transitions in ferroelectrics very precisely by not only calorimetric method but also various kinds of other methods, we have developed the "mK-stabilized cell" with a small size<sup>1-4</sup>. The outlook and the cross section of the prototype of the "cell" are shown in Figs. 1 and 2, respectively. It is based on the heat flux DSC having a high degree of temperature stability better than 1 mK as seen in Fig. 3. The block diagram of the temperature regulation system is shown in Fig. 4. The "cell" is possible to change the temperature with a quasi-static condition by an infinitesimal small rate not only on heating but also on cooling passing through the transition points. It enables us to make simultaneous measurements of endothermic heat or exothermic heat with dielectric constants, displacement currents, etc having a high degree of temperature resolution. Figure 5 is the schematic illustration of the measuring method of the displacement currents along three crystallographic axes caused by the slight displacement of atoms at the phase transitions. X-ray diffraction measurements having a thermal anomaly sensor are also possible by a minor modification of the "cell". Its cross section is shown in Fig. 6.

The method was applied to the 403 K phase transition in BaTiO<sub>3</sub> single crystal made by the TSSG method, the transition mechanism of which has been discussed for a long time due to the discrepancy of understanding depending on their experimental conditions and methods. Single crystals used were served by three different sources. These samples showed essentially the same characters except a minor difference. Endothermic heat at the transition is shown in Fig. 7 and exothermic heat in Fig. 8. The

transition nature on cooling is of not a single but two steps. The results of the dielectric constants on cooling in Figs. 9 and 10 correspond with the thermal anomalies. The displacement current flows along one axis at the second thermal anomaly on cooling as seen in Fig. 11. Resonant ultrasonic measurement using the “cell” was also carried out, developing a new excitation method of resonance<sup>5</sup>. The results very near the transition point on heating and on cooling are shown in Figs. 12 and 13, respectively. The sample does not have simple softening but change its elastic constant between two thermal anomalies at  $T_1$  and  $T_2$ . Figure 14 reveals an X-ray precession pattern, where weak extra spots are observed beside the main Bragg spots. The crystal system has been cleared in the room temperature phase below the transition point. There exist two types of structures in harmony: tetragonal and monoclinic.

The new feature of the 403 K transition has been cleared. The transition process on cooling is not so simple as has been understood so far but is a multi-step nature revealed by all the methods used. With the study by X-ray diffraction it is said that  $\text{BaTiO}_3$  does not have simple structure change on cooling from the cubic to the tetragonal with the polarization along the  $[100]$  direction due to the displacement of the body-centered ion, but changes to have two types of structures in harmony in the phase below the transition temperature.

We have also shown that the study of thermal properties of phase transition is necessary to be made by simultaneous measurements with various kinds of methods in order to have more useful information, and the cooling process must be studied keeping nearly quasi-static change because it has sometimes more meaningful information than the heating process<sup>6, 7</sup>.



Fig. 1. Outlook of the "mK-stabilized cell" with the shells out of position.

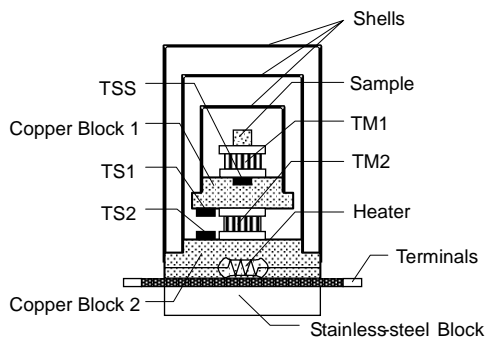


Fig. 2. Cross section of the "cell" for the precise heat flow measurement. Two coaxial copper blocks and a stainless-steel block are used as the framework. Three coaxial copper shells are tightly fixed to the copper blocks by screws. The copper blocks and a thermoelectric module of the Peltier effect are piled mutually and glued. Two coated metal-resistors connected in parallel serve as the main heater. For fine temperature regulation, the thermoelectric module TM2 is set in between the two copper blocks as the heat pump. Another thermoelectric module TM1 is for the heat flow sensor using the Seebeck effect. TS1, TS2 and TSS are temperature sensors. TS2 is near the heater and TSS is near the sample.

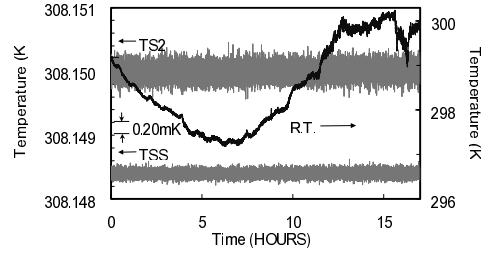


Fig. 3. Diagram showing the performance of the "cell". The temperature fluctuation, measured by TSS near the sample is  $\pm 0.20$  mK in spite of the room temperature change by 3 K.

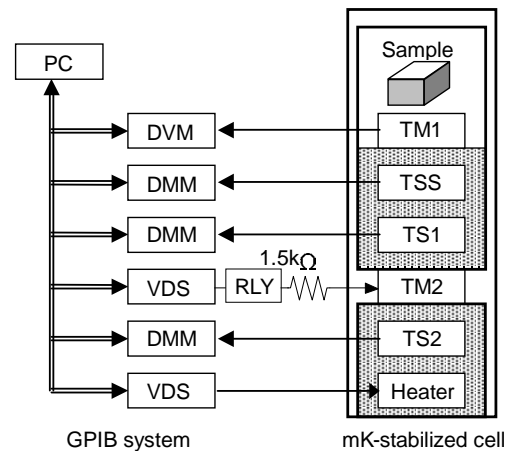


Fig. 4. Block diagram of the temperature regulation system. DVM, DMM, VDS and RL represent a digital voltmeter, a digital multi-meter, a variable DC supply and a relay connected by GPIB system, respectively. VDS has three channels; two channels for the heater and TM2, the rest channel used for the output of triggering signal to the relay in order to switch the polarity of the served voltage to TM2.

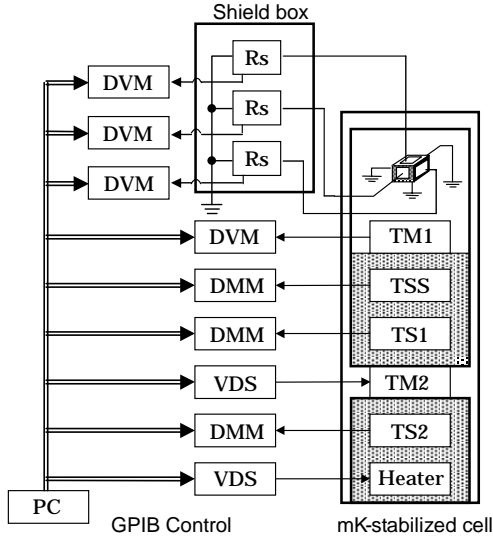


Fig. 5. Block diagram for the measurement of the displacement currents along three crystallographic directions caused by the movement of atoms at structural phase transitions, sensing heat anomalies caused by the transitions.

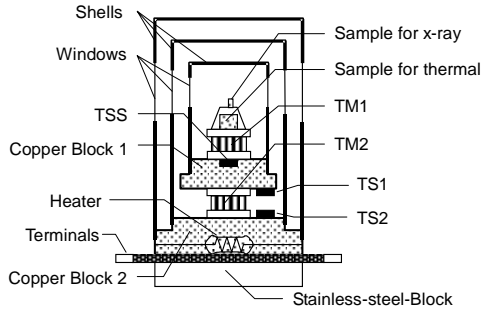


Fig. 6. Cross section of the "cell" for X-ray diffraction measurement. Each shield has windows for incident and reflected X-ray beams and is covered by superinsulator. A sample for thermal anomaly sensing is put near the sample for X-ray diffraction measurement.

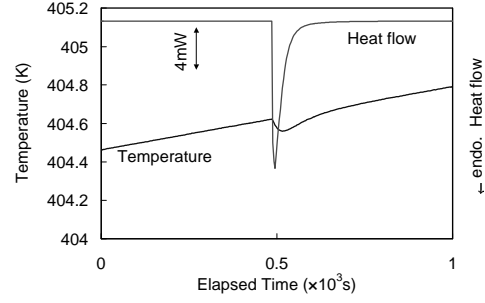


Fig. 7. Endothermic heat and the temperature on heating at the 408 K cubic-tetragonal phase transition in  $\text{BaTiO}_3$  as a function of elapsed time. The rate of temperature change is  $330 \mu\text{K/s}$ .

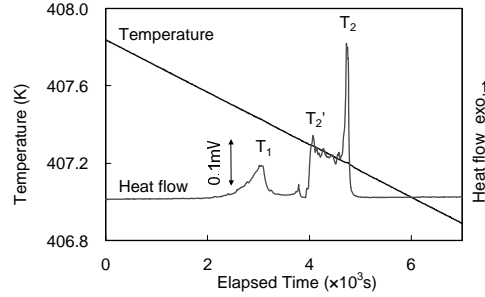


Fig. 8. Exothermic heat and the temperature on cooling at the 408 K cubic-tetragonal phase transition in  $\text{BaTiO}_3$  as a function of elapsed time.

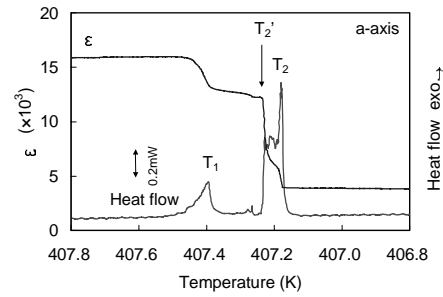


Fig. 9. Dielectric constant along the a-axis at the cubic-tetragonal phase transition on cooling in  $\text{BaTiO}_3$  at a frequency of 1 MHz and its oscillator level 0.1 V. Heat flow curve is also shown for reference.

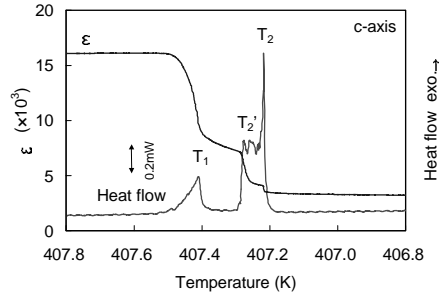


Fig. 10. Dielectric constant along the c-axis at the cubic-tetragonal phase transition on cooling in BaTiO<sub>3</sub>. Heat flow curve is also shown for reference.

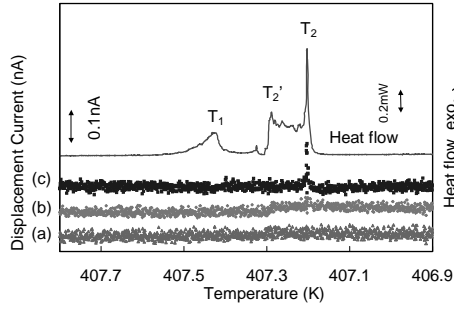


Fig. 11. Displacement currents along the three crystallographic directions at the cubic-tetragonal phase transition on cooling in BaTiO<sub>3</sub>. (a), (b) and (c) show the currents along the a-, b- and c-axes, respectively. Displacement current is observed only along the c-axis. Heat flow curve is also shown for reference.

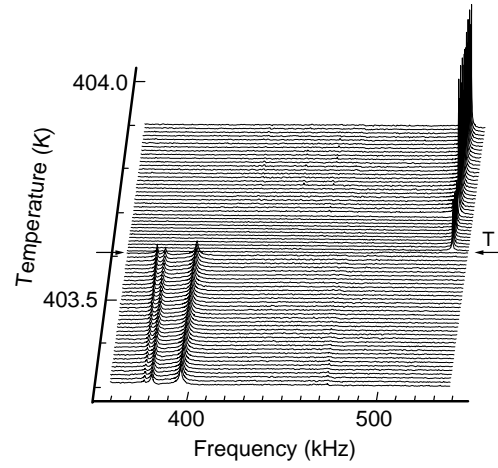


Fig. 12. Shift of the ultrasonic resonance frequency across the transition temperature on heating. The resonance peaks are shown stereographically.

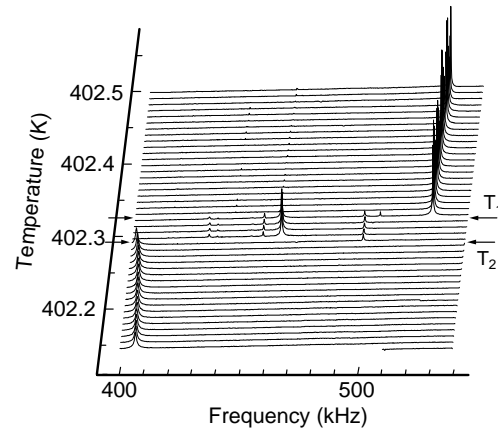


Fig. 13. Shift of the ultrasonic resonance frequency across the transition temperature on cooling. The resonance peaks are shown stereographically. It does not change in a step but includes an intermediate state between T<sub>1</sub> and T<sub>2</sub>.

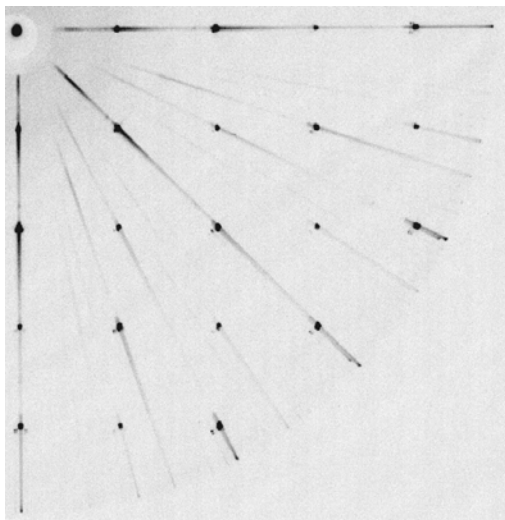


Fig. 14. X-ray precession patterns at room temperature.  
Weak extra spots are observed beside the main Bragg spots.

## References

1. A. Kojima, C. Ishii, S. Matsuda, T. Nakayama, N. Tsuda, Y. Yoshimura and H. Iwasaki, Vol. 68, 2301 (1997).
2. K. Tozaki, C. Ishii, O. Izuhara, N. Tsuda, Y. Yoshimura, H. Iwasaki, Y. Noda and A. Kojima, Rev. Sci. Instrum. Vol. 69, 3298 (1998).
3. Y. Yoshimura, A. Kojima, T. Yoshioka, Y. Kawakatsu, K. Tozaki and H. Iwasaki, Meas. Sci. Technol. Vol. 12, L.5 (2001).
4. A. Kojima, Y. Yoshimura, H. Iwasaki and K. Tozaki, Proc. Temp. Symp. 2002 (in press).
5. K. Tozaki, A. Kojima, Y. Yoshimura and H. Iwasaki, Meas. Sci. Technol. (to be submitted).
6. K. Tozaki, C. Ishii, A. Kojima, Y. Yoshimura, O. Izuhara, K. Yamada, H. Iwasaki, Y. Noda and J. Harada, Phys. Lett. A Vol. 263, 203 (1999).
7. Y. Yoshimura, K. Tozaki, A. Kojima and H. Iwasaki, Proc. SPIE vol. 4333, 18 (2001).